Studies of a Turbulent Premixed Flame Using CARS-LDV Diagnostics

Tzong H. Chen,* Larry P. Goss,† and Darryl D. Trump‡
Arvin/Calspan, Dayton, Ohio 45440
and
W. John Schmoll§
University of Dayton Research Institute, Dayton, Ohio 45469

An integrated Coherent Anti-Stokes Raman Spectroscopy/Laser Doppler Velocimetry (CARS/LDV) system was used to make temporally and spatially resolved simultaneous velocity and temperature measurements in a turbulent premixed conical flame. The reactive recirculating flow was characterized by statistical analysis of temperature and velocity data. The resulting data base is presented in the form of contour maps to facilitate quantitative and qualitative modeling evaluation. Comparison of combustion and noncombustion data was carried out to assess the effects of heat release upon the recirculating flow. Nonsteady characteristics of the flowfield were studied by means of the velocity spectra. The time scale obtained from spectral analysis was compared with the thermal time scale evaluated from the thermal balancing analysis. The ratio of these two time scales, which is equivalent to the global Damkohler number, was determined to be ~0.4 for the lean flame studied. Utilization of the combined nonintrusive laser diagnostics also allowed direct measurement of the turbulent Prandtl number.

Nomenclature

C_d = drag coefficient
C_1, C_2, C_k = shape constants
d = stabilizer base diameter
D = inner diameter of annulus duct
D_a = Damkohler number
f = frequency
L = length of recirculation zone
P_r = Prandtl number
r = radial ordinate
r_0 = radius of stabilizer base
R_0 = inner radius of annulus duct
S = surface area of recirculation zone
S_t = Strouhal number
T_f = adiabatic flame temperature
T_0 = temperature of incoming fuel-air mixture
ΔT = $T_f - T_0$
$\bar{u}$ = mean axial velocity
$\bar{u}_0$ = incoming freestream velocity
u' = root mean square (rms) of axial velocity
$\bar{v}$ = mean radial velocity
v' = rms of radial velocity
$\overline{u'v'}$ = axial velocity-radial velocity correlation
$\overline{u'T'}$ = axial velocity-temperature correlation
$\overline{v'T'}$ = radial velocity-temperature correlation
$\langle u'T' \rangle$ = axial velocity-temperature covariance
$\langle v'T' \rangle$ = radial velocity-temperature covariance
V = volume of recirculation zone
z = axial ordinate
ϵ = recirculation efficiency
ψ = stream function
τ_c = thermal characteristic time
τ_b = thermal characteristic time (reference)
τ_m = flow characteristic time

Introduction

THE mechanism of flame stabilization by a bluff body has been under intensive investigation for many years.[1-17] As a result of these studies, several parameters have been identified that affect the stability of the premixed flame stabilized by a bluff body. These parameters include stabilizer size and shape, aerodynamic blockage, pressure, upstream temperature and velocity, equivalence ratio, vitiation, freestream turbulence, and fuel properties.[1] Among these parameters stabilizer size and shape and aerodynamic blockage ratio are directly related to the stabilizer design and shall be referred to as the design parameters. The effect of stabilizer shape upon flame stabilization was taken into account by drag coefficient C_d as suggested by Barrere and Mestre.[2]

As pointed out by Beer and Chigier,[3] various experiments[4-6] have demonstrated that bluff-body flame stabilization is achieved by a continuous supply of heat carried by hot combustion products from the reverse-flow zone into the main flow. This process involves the recirculation zone, which acts as the heat source, and the surrounding shear layer, where the heat exchange occurs.[7] If flame stabilization could be assumed to be a steady-state process, then the characteristics of the recirculation zone and the surrounding shear layer could be related to the design parameters of the stabilizer.[1-17] However, recent studies of flame lifting, e.g., Chen et al.,[18] have shown that flame stabilization is a dynamic process. Some flame destabilization factors such as local flow disturbance due to azimuthal[18] or spanwise[12] inhomogeneity cannot be accounted for by the global parameters mentioned earlier. The insufficiency of using those governing parameters to account for the

Presented as Paper 88-3194 at the AIAA/ASME/SAE/ASEE 24th Joint Propulsion Conference, Boston, MA, July 11-13, 1988; received July 22, 1988; revision received Feb. 22, 1989. Copyright © 1988 American Institute of Aeronautics and Astronautics, Inc. All rights reserved.

*Senior Research Scientist, Systems Research Laboratories, Research Applications Division. Senior Member AIAA.
†Chief Scientist-Optical Diagnostics, Systems Research Laboratories, Research Applications Division. Member AIAA.
‡Project Engineer, Systems Research Laboratories, Research Applications Division.
§Associate Research Physicist, Applied Physics Division.

dynamic behavior of flame stabilization was also indicated by the experimental results of Stwalley and Lefebvre.[12] Therefore, detailed characterization of the dynamic properties of the reactive recirculating flow is warranted for an assessment of the new parameters that takes into account the dynamic flame stabilization processes.

Some dynamic features of the turbulent reacting flow have been accounted for by cross correlations of velocity and scalars. Recent developments in integrated optical diagnostic instruments have allowed the measurement of scalar-vector correlations. In the present investigation, an integrated CARS-LDV diagnostic system[19] was utilized for measuring the temperature and velocity correlations of a methane-air premixed flame stabilized by a conical bluff body. Independent and simultaneous temperature and velocity measurements were made. The flowfield was then mapped two dimensionally by means of the statistical properties of velocity and temperature. A nonreacting flow with the same inlet velocity was also mapped by velocity measurements to permit the effects of combustion upon the recirculation flowfield to be examined. The turbulent exchange of energy across the boundary of the recirculation zone was directly measured, and the values were used in performing a thermal-balancing analysis. The thermal time scale obtained from this analysis was then compared to the flow time scale obtained from spectral analysis of the velocity data. As a result, a global Damkohler number and turbulent Prandtl numbers were determined. This study will aid in the evaluation of time-averaged and/or time-dependent computational models of the reacting flowfield which, in turn, may help reduce cut-and-try efforts in the design process.

Experimental

Flow Configuration

A schematic diagram of the conical stabilizer flow system is shown in Fig. 1a. The premixed methane-air flame was stabilized by a 45-deg conical stabilizer of base diameter $d = 45$ mm, mounted coaxially at the exit plane of a circular pipe of inner diameter $D = 80$ mm. This circular pipe supplied a premixed methane-air mixture from a vertical combustion tunnel mounted on a three-axis traversing platform.

The methane and air were mixed at an equivalence ratio of 0.57, which yielded an adiabatic flame temperature of 1600 K. The inlet velocity of the mixture at the exit plane of the bluff body was 10 m/s, which closely approaches the lean blowout condition. Blowout will occur with further increase in inlet velocity. With the freestream velocity of 10 m/s, the resulting shear layer surrounding the recirculation zone consists of coherent structures. The effects of these structures upon the turbulent heat exchange between the recirculation zone and approaching freestream through the shear layer can be investigated. Figure 1b is a photograph of a bluff-body-stabilized reacting flowfield. TiO_2 particles from $TiCl_4$-H_2O reactions were seeded into the freestream mixture to permit the interface between the hot flame zone and the cold reactant to be viewed. In this photograph, the coherent structures of the interface can be clearly seen.

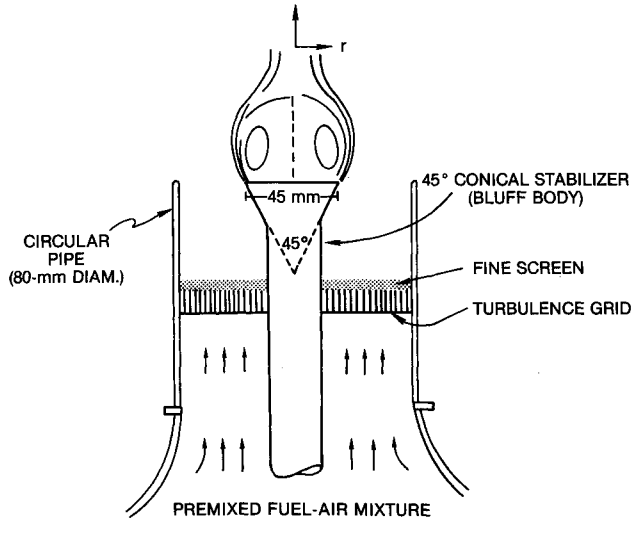

Fig. 1a Schematic diagram of axisymmetric premixed flame burner with 45-deg conical stabilizer ($d = 45$ mm).

CARS-LDV System

The combined CARS-LDV[20-21] system is shown schematically in Fig. 2. Since details of this system were given in Ref. 19, only the salient features will be mentioned here. In the CARS system the frequency-doubled output from a Quanta-Ray DCR-2 Nd:YAG laser was used to pump a broadband dye laser and was also used as the pump frequency in the CARS process. Maximum spatial resolution was achieved by reducing the intersection volume of the pump and probe beams via a folded BOXCARS[22] arrangement. The length of the probe volume along the major beam axis was measured to be 0.8 mm. Time resolution of the CARS instrumentation is 10 ns, which is the width of the laser pulse. The receiving optics utilize a splitter arrangement to extend the dynamic range of the detector, which allows study of the temperature in the range 300–2300 K. At low temperature the CARS system typically displays a precision for repeated single-shot temperature measurements of 80 K and an accuracy in time-averaged temperature measurements of 10 K. In the high-temperature region, the signal from the hot band of the CARS spectra is strong and results in a precision of <60 K.

The LDV system was built by Lightman et al.[23] and is a two-component real-fringe system based on polarization sepa-

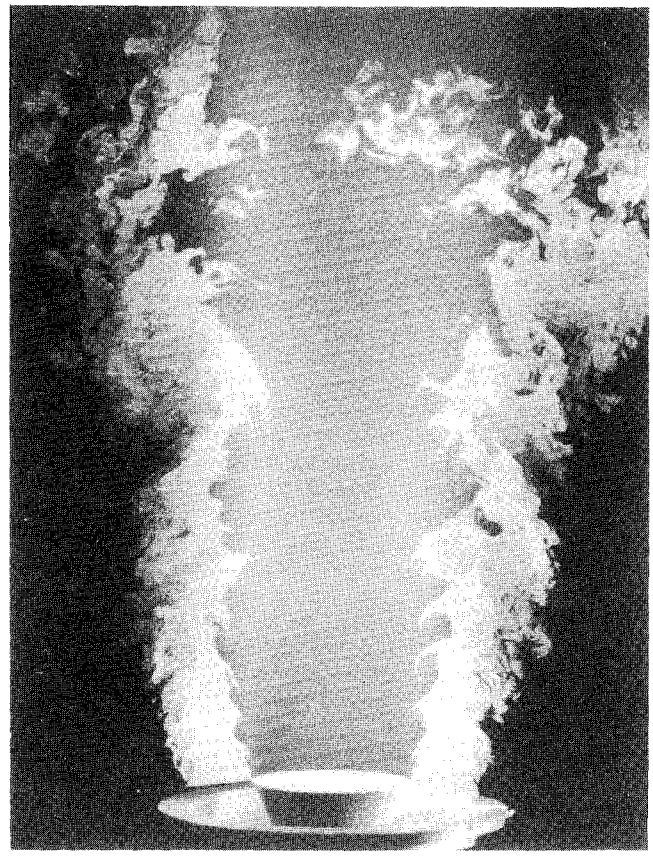

Fig. 1b Premixed flame stabilized by conical stabilizer.

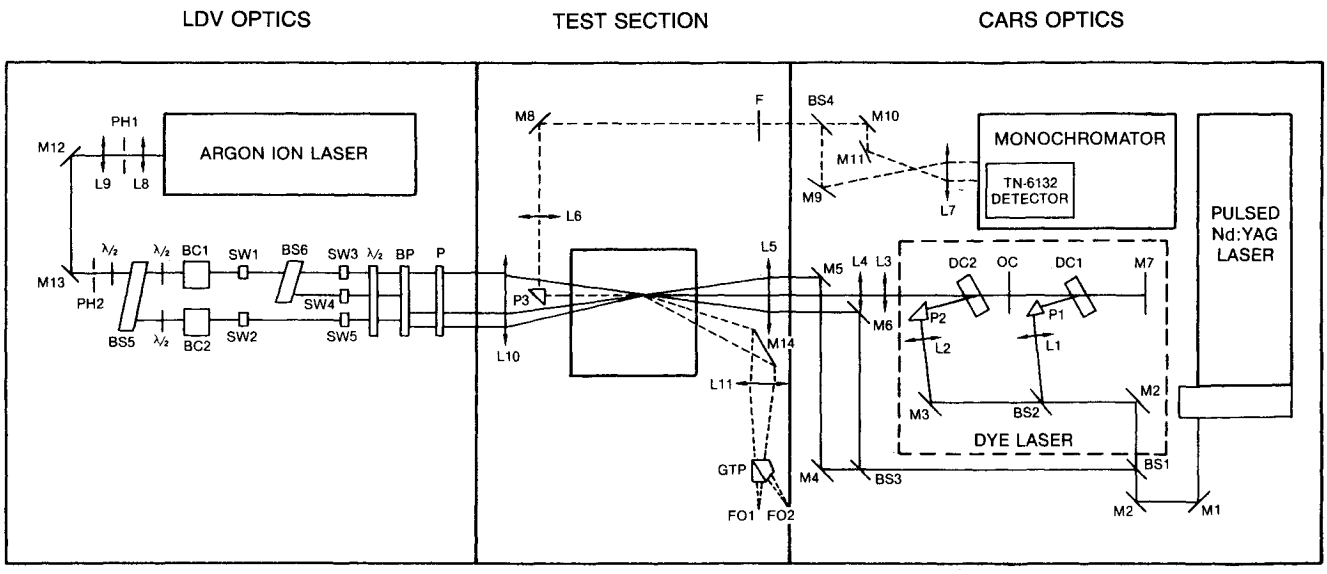

Fig. 2 Optical arrangement of integrated CARS-LDV instruments.

ration of the velocity components. The 514.5-nm line from a Spectra-Physics argon-ion laser was used as the light source, with 0.5-μm-diameter alumina (Al_2O_3) particles serving as the scattering medium. The Doppler burst was collected in the forward direction slightly off-axis (= 10 deg). Dual Bragg cells having a 5-MHz frequency difference were employed to remove directional ambiguities and maintain the Doppler burst frequencies in an optimum range for the velocities under study.

The CARS and LDV instruments were aligned head-on. Since they have no common optics, they can be operated separately or jointly without interference. Three LDV beams and three CARS beams were crossed and aligned through a 100-μm aperture. The simultaneity of the CARS and LDV measurements was achieved jointly by hardware interfaces and software. For joint CARS-LDV measurements, a common clock is used; when a measurement is made, both temperature and velocity data are tagged with time. Three operational modes are available.[19] One of these modes allows an optimum coincidence time of 4 μs; however, an extremely low sampling rate results from the use of this narrow window. Therefore, for the present study the width of the window was set at 250 μs; thus, the value of simultaneity was ~100 μs on the average, with a data-sampling rate of ~3 Hz. This simultaneity was adequate for correlating the temperature and velocity for the reacting flowfield studied, which had a reference velocity of 10 m/s and a dominant frequency of <600 Hz. Due to the lower coincidence rate 1500 joint data points were taken at each measurement location. Higher data rates are possible with a higher-density seed; however, this increases the possibility of particle breakdown, which will invalidate the CARS data.

For the independent measurements, the CARS instrumentation takes data at a 10-Hz rate and the LDV at an average rate of 2000–4000 Hz. Therefore, 4096 data points were recorded at each measurement location. Except for the joint temperature and velocity data presented in the last part of the Results and Discussion Section, all the velocity and temperature data presented were taken independently. Statistically, using 4096 data points, the associated standard error for the averages and standard deviations is $1/\sqrt{4096}$ (= 1.56%). The data were statistically analyzed, resulting in mean, root mean square (rms), skewness, kurtosis, correlation coefficients, Reynolds stresses, joint probability distribution functions (PDF), and conditional averages. Radial scans were made at more than 10 axial locations for the construction of the contours presented in this paper.

Results and Discussion

Due to the massive amounts of data acquired by the computerized data acquisition system, only those results that help explain the major observations of the flame studied will be presented here. Detailed data such as inlet velocity and temperature profiles have been documented following the suggestion of Strahle,[24] Libby et al.,[25] and Sturgess et al.[26] In this section the velocity statistics for the reacting and nonreacting flowfields are presented, followed by the temperature statistics for the reacting flowfield. Next, information on the spectral analysis of the velocity field inside the recirculation zone is given. Finally, the joint velocity-temperature measurements are discussed.

Velocity Statistics for Reacting and Nonreacting Cases

Knowledge of the flow pattern in the bluff-body recirculation zone is important to the understanding of flame stabilization.[3,4,7,10,13] Contours of various velocity statistics are presented in this section to depict the main features of the flow pattern. The noncombusting and combusting results are shown side by side to facilitate direct comparison for assessing the effects of combustion upon the turbulent flowfield.

One method of displaying the flow pattern is to measure the stream function, defined as[27]

$$\psi = \int_0^r \bar{u} \cdot r \, dr \Big/ \int_0^{R_0} \bar{u} \cdot r \, dr \qquad (1)$$

representing the volume flow rate, where $\bar{u}$ is the axial velocity and R_0 is the radius of the annulus duct. From this definition the total volume flow is 1.0. Figures 3a and 3b show the stream function of cold and combusting flows. The velocity vectors of these flows are shown in Figs. 4a and 4b, respectively. The minimum value of the stream function defined in Eq. (1) is −0.077 for the cold flow and −0.126 for the combusting flow, indicating that the recirculated flow volume for the combusting flow is about twice that for the cold flow. Consequently, the length L of the recirculation zone is increased from 52 mm (L/d = 1.15) for the cold flow to 98 mm (L/d = 2.17) for the combusting flow. The volume-flow increases via thermal expansion due to combustion should be more than tripled. The fact that the volume is doubled rather than tripled means that the mass entrained into the recirculation zone for the combustion flow is less than that entrained for the cold flow. This reduced entrainment is consistent with the fact that

the inward radial velocity for the combusting flow is smaller than that for the cold flow, as will be shown in Figs. 6a and 6b.

The mean velocity results can also be used to indicate the recirculation efficiency ϵ of a flame holder by defining ϵ as

$$\epsilon = \max\left[-\int_0^r \bar{u} \cdot r \, dr \Big/ (\bar{u}_0 \cdot r_0^2) \right] \Big|_0^{r_0} \qquad (2)$$

where $\bar{u}_0$ is the incoming freestream velocity and r_0 the radius of the bluff body. By this definition, the recirculation efficiency is 18% for the cold flow and almost doubled to 35% for the combusting flow.

Figures 5a and 5b show the contours of the axial velocity for the cold and combusting flowfield. The contours of the radial velocity are shown in Figs. 6a and 6b. The rms values of the axial and radial velocity fluctuations are shown in Figs. 7 and 8, respectively. Reynolds stresses were represented by the value of the correlation coefficients and are shown in Fig. 9. After examination and comparison of Figs. 3–9, a general observation can be made. Inside the recirculation zone, the velocity field contains two stagnation points—one corresponding to the center of the toroidal vortex core and the other representing the tip of the recirculation zone (see Figs. 3a and 3b). Thus, the velocity field is very complicated and contains a variety of interesting features associated with these two stagnation points.

Comparison of noncombustion and combustion data indicates that combustion has doubled the length of the recirculation zone and increased the magnitude of the maximum reversed axial velocity from 3.9 to 6.0 m/s (compare Figs. 5a and 5b). Although the velocity contours are stretched axially by combustion, the shapes are very similar, as can be seen from Figs. 3–6. The radial velocity measurements have exhibited some striking results relative to the flame affecting the flow entrainment. The maximum outward radial velocity of 2.1 m/s was found to occur near the tip of the bluff body for both the combusting and noncombusting cases. This can be explained by the geometry and inlet velocity being the same for both cases. However, the maximum magnitude of the inward radial velocity is 2.8 m/s for the cold flow and 1.4 m/s for the combusting flow. This maximum entrainment occurs at the axial station where the end of the recirculation zone is located (see Figs. 6a and 6b). The decreases of the inward radial velocity may be due to several adverse effects that reduce the entrainment. First, thermal expansion has a tendency to expand the volume of the hot products inside the recirculation zone and create an outward velocity that will suppress the inward velocity. Secondly, the temperature gradient due to the flame is

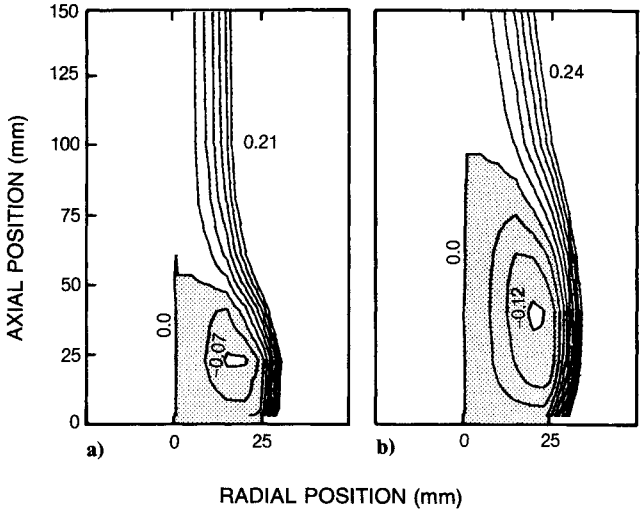

Fig. 3 Measured stream functions for a) cold flow and b) reacting flow.

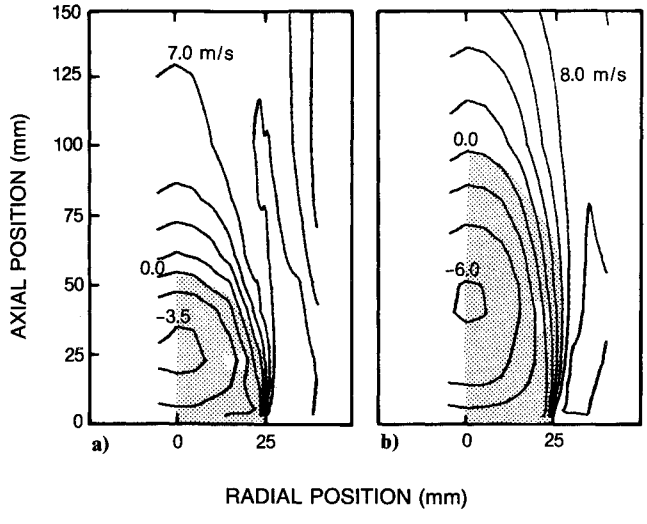

Fig. 5 Measured contours of axial velocity for a) cold flow and b) reacting flow.

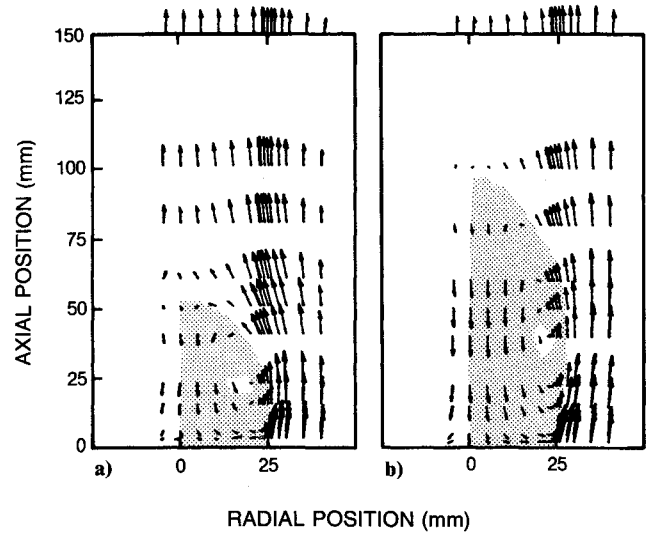

Fig. 4 Measured velocity vectors for a) cold flow and b) reacting flow.

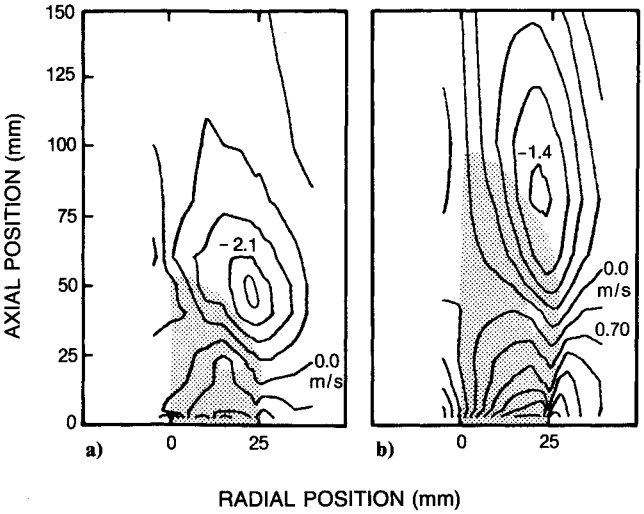

Fig. 6 Measured contours of radial velocity for a) cold flow and b) reacting flow.

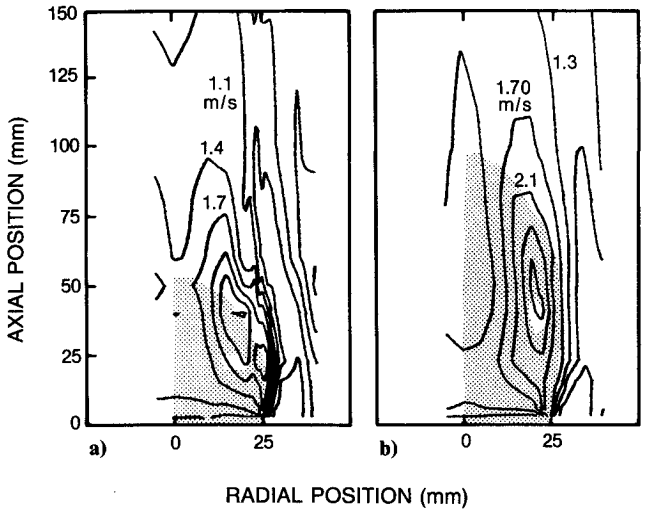

Fig. 7 Measured contours of rms axial-velocity fluctuations for a) cold flow and b) reacting flow.

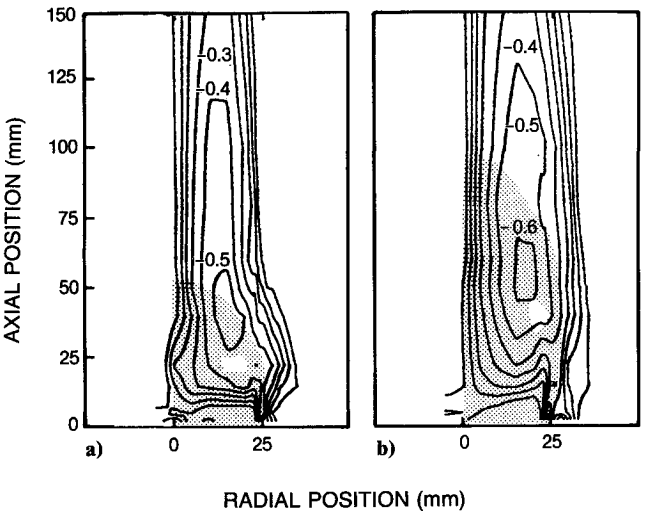

Fig. 9 Contours of correlation coefficients of axial and radial velocity for a) cold flow and b) reacting flow.

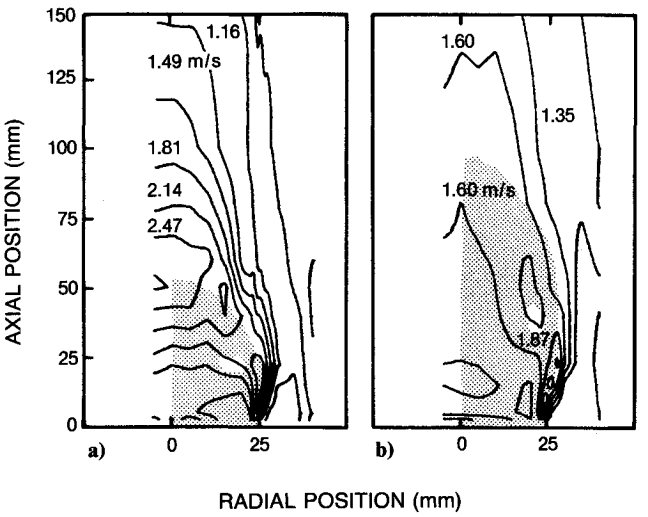

Fig. 8 Contours of rms radial-velocity fluctuations for a) cold flow and b) reacting flow.

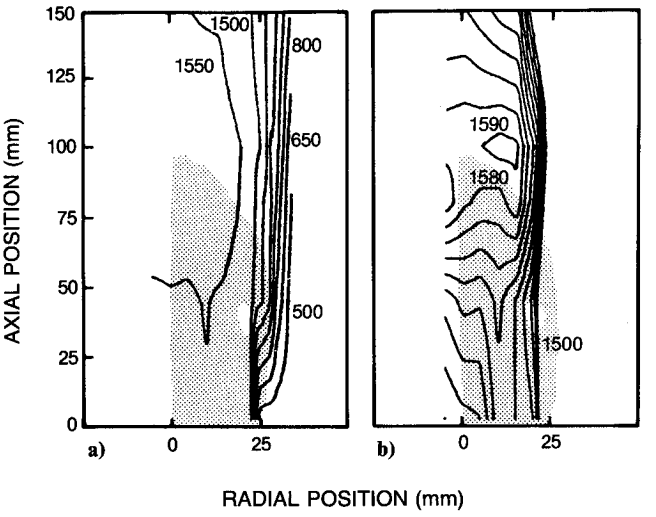

Fig. 10 Contour of mean temperature in range a) 500–1550 K and b) 1500–1590 K.

opposed to the axial-velocity gradient and will cause a reduction in the strength of the vortex, which is driven by the velocity gradient. In addition, the increased kinematic viscosity will further reduce the local vortex strength to reduce the vortex-induced entrainment.

The magnitude of the rms velocity for the axial and radial components is not significantly affected by combustion. The maximum rms axial velocity u' for the cold flow is 2.62 m/s and increases to 2.99 m/s for the combusting flow. On the other hand, the maximum rms radial velocity v' for the cold flow is 2.83 m/s and decreases to 2.44 m/s for the combusting flow. Note that combustion has reduced the value of v' at the tip of the recirculation zone from 2.6 m/s for the cold flow to 1.8 m/s for the combusting flow. This amounts to a 30% reduction of v' due to combustion.

The contours of the Reynolds stresses, shown in the form of correlation coefficients, exhibit a strong similarity between the cold flow and the combusting flow. The maximum magnitude of the correlation coefficients is -0.54 for the cold flow and -0.60 for the combusting flow. This high correlation is because the flow is dominated by two-dimensional features of the toroidal vortex. For the swirling flow, which is highly three-dimensional, the correlation coefficient is measured to be ~ 0.25.[27] The contour of the maximum correlation is stretched significantly away from the area downstream of the core of the toroidal vortex. The area enclosed by the stretched maximum contour line may be the area through which the shed toroidal vortex travels. By comparing Figs. 9a and 9b it is found that the route taken by the shed toroidal vortex is very similar for the cold and combusting flows.

Temperature Statistics

The contours of the mean and rms temperatures are shown in Figs. 10 and 11. Unlike the complicated velocity flowfield, the temperature inside the recirculation zone is uniform at ~ 1500 K. This observation confirms the assumption that the thermal field behind a bluff body is well mixed and uniform. This could be associated with the fact that the flame front only brushes the shear-layer region surrounding the recirculation zone and, after crossing the flame brush, the recirculated gas consists mainly of burned hot products. The difference between this temperature and the adiabatic flame temperature, 1600 K for the mixture applied in this study, is around 100 K and confirms the observations made by other researchers.[1] The contours of rms temperature shown in Fig. 11 also indicate that the temperature fluctuation is smaller than 100 K inside

the recirculation zone. The maximum temperature fluctuation is ~600 K and occurs in the flame-brushing area in the same axial location as the tip of the recirculation zone (one of the stagnation points). At the same axial location, the radial velocity reaches its minimum value of −1.4 m/s, which indicates maximum entrainment. The ample entrainment of fresh mixture into the stagnation point maintains a local higher temperature regime, as shown in Fig. 10b. In this figure, temperature contours in the temperature range 1500–1600 K give a more detailed picture of the temperature profile inside the recirculation zone. The more detailed temperature fluctuation ranging from 60 to 100 K is shown in Fig. 11b. This figure indicates that the temperature fluctuation actually reaches its minimum around the core of the recirculation zone and yet pertains to a large v', as shown in Fig. 8b.

The effects of flame brushing on the thermal field can be demonstrated by the PDF of the temperature across the flame zone. Figures 12a–12d show the temperature PDFs along the radial direction at various downstream locations. Inside the flame zone, the temperature statistics showed distinct bimodal distributions as a result of flame brushing. However, the velocity field showed no evidence of bimodal distribution. This implies that the velocity and temperature are transported with different "efficiencies" across the sheared flame zone via the coherent structures as well as flame flapping.

From these PDF contours, it is found that away from the bluff body the maximum temperature is populated ~1500 K inside the recirculation zone and rises to ~1600 K at the flame zone. However, in the flame zone, the intermittency results in a mean temperature lower than that in the inward area adjacent to the flame. Near the bluff-body surface, $z = 2.5$ mm, the maximum temperature is populated at a lower value around 1450 K. Therefore, along the flame brush, the temperature peaks at a location away from the edge of the bluff body. The local maximum temperature is referred to as the temperature bulge,[28] and its appearance indicates the occurrence of flame development. Other factors contributing to a lower maximum temperature are as follows: 1) the velocity gradient is highest near the edge of the bluff body and the flame might be subjected to larger stretching along the flame surface, 2) the temperature gradient is also highest, and 3) heat is being transferred to the bluff body. As a result, convection and conduction both contribute to the temperature being at a lower maximum value.

Spectral Analysis

The unsteadiness of the reacting flow behind the bluff body can be characterized by temperature and/or velocity fluctua-

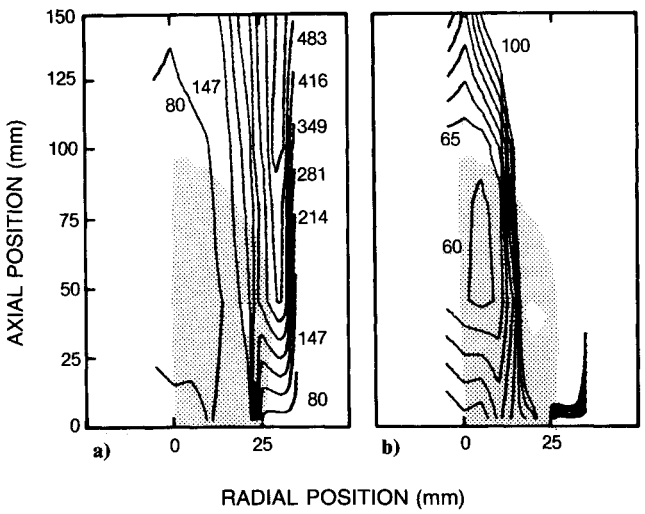

Fig. 11 Contours of rms temperature fluctuation in range a) 80–550 K and b) 60–100 K.

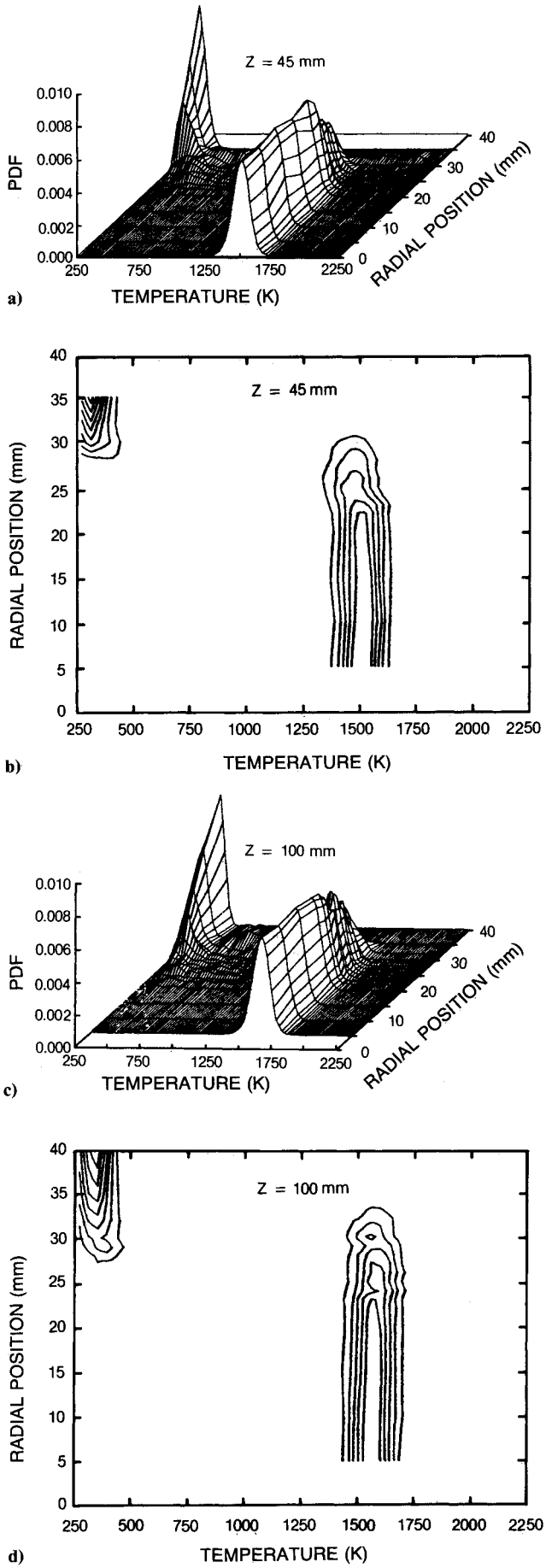

Fig. 12 Three-dimensional plots and associated contours of temperature PDF's at various radial positions for a,b) $z = 45$ mm, c,d) $z = 100$ mm.

tions. Since the temperature is measured to be rather uniform and velocity to be strongly fluctuating, the spectra of the velocity fluctuations are used to show the flow unsteadiness. For spectral analysis, velocity data were taken independently of temperature data to achieve a high sampling rate, 2000–4000 Hz. Figure 13 shows the velocity spectra along the axial locations $z/d = 0.66$ and 2.22. At $z/d = 0.66$, the velocity spectra exhibit two peaks corresponding to frequencies of 15 and 40 Hz. At $z/d = 2.22$, near the end of the recirculation zone, only one spectral peak occurs, corresponding to a frequency of 40 Hz. This distinct peak corresponds to the unsteady oscillation with a Strouhal Number $St = fd/u_0$ of 0.18, where f is the frequency, d the fluff-body diameter, and u_0 the mean annulus inlet velocity. This Strouhal number agrees with values observed[17,29] for vortex shedding ranging between 0.18 and 0.22.

Near the nozzle tip, the initial vortex is smaller (see Fig. 2b) and has a shedding frequency at 580 Hz, which is very close to the initial frequency of an axisymmetric air jet with a jet velocity of 8.0 m/s. After the reactant mixture flows through the flame brush and circulates into the recirculation zone, it loses its initial shear-layer identity. The frequency of 40 Hz is much lower than the initial frequency and corresponds to the shedding (or circulating cycle) of the toroidal vortex, which is the core of the recirculation zone. The flow characteristic time $\tau_m = 25$ ms (1/40 Hz) can then be considered as the time required by the flow to refresh the recirculation zone.

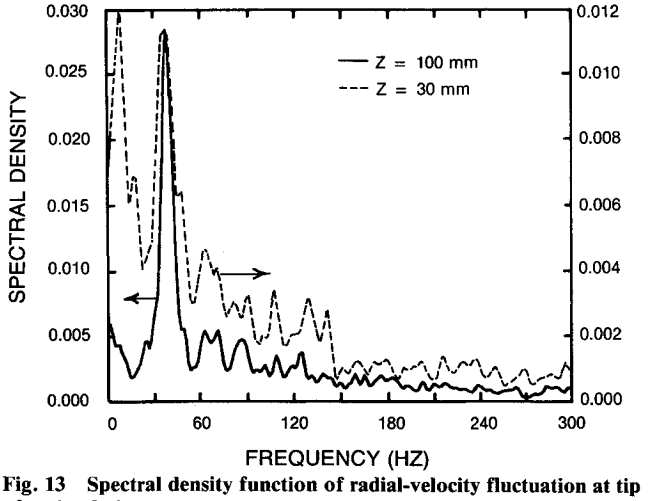

Fig. 13 Spectral density function of radial-velocity fluctuation at tip of recirculation zone.

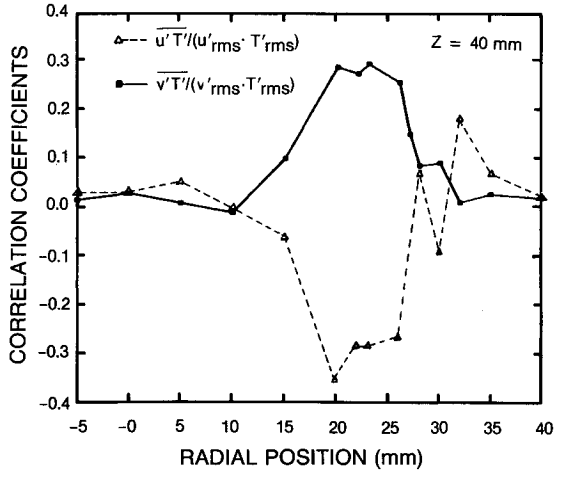

Fig. 14 Measured correlation coefficients for temperature and velocity, radial scans at $z = 40$ mm.

Joint Temperature and Velocity Measurement

Figure 14 shows the measured velocity-temperature covariances $\langle u'T' \rangle$ and $\langle v'T' \rangle$. These covariances are the normalized correlation coefficients of the velocity-temperature correlations $\overline{u'T'}$ and $\overline{v'T'}$. Since the joint correlations $\overline{u'T'}$ and $\overline{v'T'}$ are the measure of the turbulent exchange of the thermal property across the flame zone, the characteristic time required for the flow inside the recirculation zone to be refreshed can be estimated by the heat-balance analysis as follows. In this analysis the surface S and volume V of the recirculation zone are involved. These two quantities can actually be computed from the measured contours of the stream function shown in Fig. 3. However, for dimensional analysis purposes, let us use the radius of the bluff body r_0 and the length of the recirculation zone L to compute the surface and the volume as

$$\text{surface area:} \quad S = C_1 \cdot (2\pi r_0) \cdot L$$

$$\text{volume:} \quad V = C_2 \cdot (\pi r_0^2) \cdot L \tag{3}$$

The thermal characteristic time τ_c can be defined as

$$\tau_c \equiv (\text{volume} \cdot \Delta T)/(\text{surface area} \cdot \overline{v'T'})$$

$$= [V \cdot (T_f - T_0)]/(S \cdot \overline{v'T'}) \tag{4}$$

Combining Eqs. (3) and (4), one obtains

$$\tau_c = [C_2 r_0 (T_f - T_0)]/(C_1 \cdot 2 \cdot \overline{v'T'})$$

$$\equiv C_k \cdot \tau_b \tag{5}$$

where $C_k = C_2/C_1$ is a shape constant. The remainder of the terms on the right-hand side of Eq. (5) have the same unit as time and are designated as τ_b. The value of this time scale was 0.066 s using the measured value of $\overline{v'T'}$, which is typically 200 (m/s·K) in the flame zone. As shown previously, the flow characteristic time τ_m is 0.025 s. Therefore, the value of C_k is 0.38, provided the flow time is equal to the thermal time. Consequently, this measured constant can be used to estimate the turbulence exchanges, provided their direct measurement is not possible. In this analysis the length of the recirculation zone L is cancelled. This implies that the aerodynamic performance of the bluff body can be characterized by the bluff-body diameter and a shape factor related to the bluff-body design parameters. If the value of $\overline{u'T'}$ is used instead of $\overline{v'T'}$ in the preceding calculation, C_k will be 0.6. The value of C_k in the range 0.38–0.60 is of the same order as the value of the drag coefficient C_d. Thus, one may conclude that Barrere and

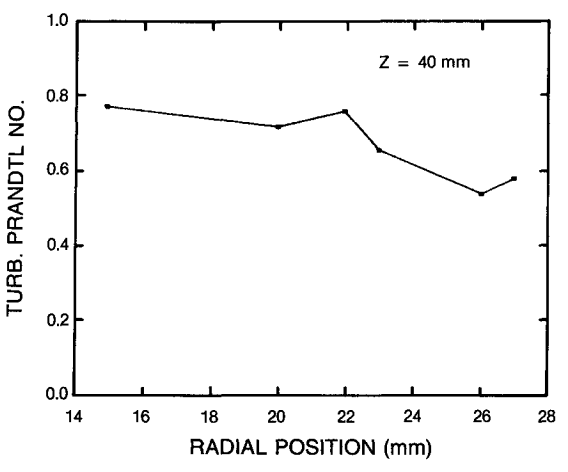

Fig. 15 Measured turbulent Prandtl number across flame at $z = 40$ mm.

Mestre's[2] approach to the use of C_d to govern the shape factor is indeed a valid one.

The Damkohler number, which is the ratio of the flow mixing time and the chemical reaction time,

$$D_a = \tau_m / \tau_b \tag{6}$$

has been related to the flame stabilization criterion.[1,9,10] For the lean flame studied, the global Damkohler number defined in Eq. (6) is measured to be ~0.4. Since the flame was operated in the near-blowout regime this value may be a critical Damkohler number for flame blowout.

In modeling the reacting flow the value of the turbulent Prandtl number is needed to relate the transport of the thermal property to that of the momentum. The turbulent Prandtl number is defined as the ratio of the momentum diffusivity to the thermal diffusivity,[30]

$$P_r = [\overline{u'v'}/(\delta u/\delta r)]/[\overline{v'T'}/(\delta T/\delta r)] \tag{7}$$

This number can be measured directly since all the terms in Eq. (7) are directly measurable by the integrated CARS-LDV technique. Figure 15 shows the profile of the turbulent Prandtl number at an axial location of $z = 40$ mm where the toroidal vortex is located at the same height. Across the flame-brush region the measured Prandtl number, which ranges from 0.55 to 0.8, is less than unity. Thus, the turbulent momentum diffusivity is smaller than the turbulent thermal diffusivity in this region.

Conclusions

The combined CARS-LDV technique has been shown to be an ideal tool in the study of the reactive recirculating flowfield. In spite of the high degree of technical difficulty and very low sampling rate, its capability to provide precise and simultaneous temperature-velocity data makes it a good instrument for generating a benchmark-quality database. Its ability to distinguish measurement bias due to LDV seeding and perform conditional sampling has been realized. The results analyzed by conditional sampling will be reported in the near future.

The following conclusions were drawn concerning the character of recirculating flows:

1) Inside the recirculation zone, the velocity field contained two stagnation points—one corresponding to the center of the toroidal vortex core and the other representing the tip of the recirculation zone. The temperature distribution was found to be uniform inside this zone. However, near the tip of the recirculation zone, the temperature is slightly higher than in the other locations.

2) Comparison of combustion and noncombustion data indicates that combustion has doubled the length of the recirculation zone and increased the magnitude of the maximum reversed axial velocity from 3.9 to 6.0 m/s. Although the velocity contours have been stretched axially by combustion, the shapes are very similar.

3) The entrainment of freestream gas into the recirculation zone has been reduced by the occurrence of combustion. The maximum inward radial velocity for the cold flow is 2.8 m/s and decreases to 1.4 m/s for the combusting flow.

4) In the flame-brushing region, the turbulent heat fluxes are highest, and the maximum magnitude of the correlation coefficients for velocity and temperature is ~0.35. The maximum magnitude of the correlation coefficient for the axial and radial velocity is ~0.6.

5) Inside the flame zone, temperature statistics showed distinct bimodal distributions as a result of flame brushing. However, the velocity field showed no evidence of bimodal distribution. This implies that the momentum and heat are transported differently across the sheared flame brush. As a result, the turbulent Prandtl number was measured to be less than unity. The measured turbulent Prandtl numbers are in the range 0.55–0.8.

6) The toroidal vortex is shed at 40 Hz. The associated characteristic time is then 0.025 s. The thermal characteristic time is measured to be 0.066 s. This results in a global Damkohler number of ~0.4. This may be the critical Damkohler number for the lean blowout because the flame was operated in a lean blowout regime.

Acknowledgments

This work is supported by the Air Force Wright Aeronautical Laboratories, Aero Propulsion Laboratory, under Contracts F33615-85-C-2562 (Systems Research Laboratories) and F33615-87-C-2767 (University of Dayton). The authors are indebted to W. M. Roquemore for helpful suggestions concerning this work and to M. Whitaker, J. Heinrichs, J. Stutrud, and C. Obringer for technical assistance.

References

[1]DeChamplain, J. A. and Bardon, M. F., "A Model for Bluff Body Flame Stabilization," American Society of Mechanical Engineers, Paper 86-GT-155, June 1986.

[2]Barrere, M. and Mestre, A, "Stabilization des Flames par des Obstacles," *AGARD Selected Combustion Problems—Fundamentals and Aeronautical Applications,* Butterworths Scientific Publications, London, 1954, pp. 426–446.

[3]Beer, J. M. and Chigier, N. A., *Combustion Aerodynamics,* Wiley, New York, 1972.

[4]Williams, G. C., Hottel, H. C., and Scurlock, A. C., "Flame Stabilization and Propagation in High Velocity Gas Streams," *Third Symposium (International) on Combustion,* Williams and Wilkins, Baltimore, MD, 1949, pp. 21–40.

[5]Spalding, D. B., "Theoretical Aspects of Flame Stabilization—An Approximate Graphical Method for the Flame Speed of Mixed Gases," *Aircraft Engineering,* Vol. 25, Sept. 1953, pp. 264–268.

[6]Zukoski, E. E. and Marble, F. E., "The Role of Wake Transition in the Process of Flame Stabilization on Bluff Bodies," *AGARD Combustion Research and Reviews,* Butterworths, London, 1955, pp. 167–180.

[7]Bovina, T. A., "Studies of Exchange Between Re-circulation Zone Behind the Flame-Holder and Outer Flow," *Seventh Symposium (International) on Combustion,* The Combustion Institute, Pittsburgh, PA, 1959, pp. 692–696.

[8]Winterfeld, G., "On Processes of Turbulent Exchange Behind Flame Holders," *Tenth Symposium (International) on Combustion,* The Combustion Institute, Pittsburgh, PA, 1965, pp. 1265–1275.

[9]Plee, S. L. and Mellor, A. M., "Characteristic Time Correlation for Lean Blowoff of Bluff-Body-Stabilized Flames," *Combustion and Flame,* Vol. 35, May 1979, pp. 61–80.

[10]Radhakrishnan, K., Heywood, J. B., and Tabaczynski, R. J., "Premixed Turbulent Flame Blowoff Velocity Correlation Based on Coherent Structures in Turbulent Flows," *Combustion and Flame,* Vol. 42, July 1981, pp. 19–33.

[11]Strehlow, R. A. and Malik, S., "The Mechanisms of Flame Holding in the Wake of a Bluff Body," NASA CR 3866, March 1985.

[12]Stwalley, R. M., III and Lefebvre, A. H., "Flame Stabilization Using Large Flameholders of Irregular Shape," AIAA Paper 87-0469, Jan. 1987.

[13]Kundu, K. M., Banerjee, D., and Bhaduri, D., "On Flame Stabilization by Bluff-Bodies," *Journal of Engineering for Power,* Vol. 102, Jan. 1980, pp. 209–214.

[14]Fujii, S. and Eguchi, K., "A Comparison of Cold and Reacting Flows Around a Bluff-Body Flame Stabilizer," *Journal of Fluids Engineering,* Vol. 103, June 1981, pp. 328–334.

[15]Rao, K. V. L. and Lefebvre, A. H., "Flame Blowoff Studies Using Large-Scale Flameholders," *Journal of Engineering for Power,* Vol. 104, Oct. 1982, pp. 853–857.

[16]Taylor, A. M. K. P. and Whitelaw, J. H., "Velocity Characteristics in the Turbulent Near Wakes of Confined Axisymmetric Bluff Bodies," *Journal of Fluid Mechanics,* Vol. 139, Feb. 1984, pp. 391–416.

[17]Roquemore, W. M., Bradley, R. P., Stutrud, J. S., Reeves, C. M., Britton, R. L., Sandhu, S. A., and Archer, R. S., "Influence of the Vortex Shedding Process on a Bluff-Body Diffusion Flame," AIAA Paper 83-0335, Jan. 1983.

[18]Chen, T. H. and Goss, L. P., "Flame Lifting and Flame/Flow Interactions of Jet Diffusion Flames," AIAA Paper 89-0156, Jan. 1989.

[19]Goss, L. P., Trump, D. D., Lynn, W. F., Chen, T. H., Schmoll, W. J., and Roquemore, W. M., "Second-Generation Combined CARS-LDV Instrument for Simultaneous Temperature and Velocity Measurements in Combusting Flows," *Review of Scientific Instruments,* Vol. 60, No. 4, 1989, pp. 638–645.

[20]Fujii, S., Gomi, M., and Eguchi, K., "A Remote Laser-Probe System for Velocity and Temperature Measurement," *Journal of Fluids Engineering,* Vol. 105, June 1983, pp. 128–133.

[21]Goss, L. P., Trump, D. D., and Roquemore, W. M., "Combined CARS/LDA Instrument for Simultaneous Temperature and Velocity Measurements," *Experiments in Fluids,* Vol. 6, March 1988, pp. 189–198.

[22]Eckbreth, A. C., *Laser Diagnostics for Combustion Temperature and Species,* Abacus Press, Tunbridge Wells, United Kingdom, 1988.

[23]Lightman, A., Magill, P. D., and Andrews, R. J., "Two-Dimensional Laser Doppler Anemometer Studies of Isothermal Flowfield in a Ducted Center-body Combustor," AFWAL-TR-83-2044, Air Force Wright Aeronautical Laboratories, Wright-Patterson Air Force Base, Ohio, June 1983.

[24]Strahle, W. C., "Preface to 'Evaluation of Data on Simple Turbulent Reacting Flows,' " *Progress in Energy and Combustion Science,* Vol. 12, 1986, pp. 253–255.

[25]Libby, P. A., Sivasegaram, S., and Whitelaw, J. H., "Premixed Combustion," *Progress in Energy and Combustion Science,* Vol. 12, 1986, pp. 393–405.

[26]Sturgess, G. J., Syed, S. A., and McManus, K. R., "Importance of Inlet Boundary Conditions for Numerical Simulation of Combustion Flows," AIAA Paper 83-1263, June 1983.

[27]Brum, R. D. and Samuelsen, G. S., "Two-Component Laser Anemometry Measurements of Non-Reacting and Reacting Complex Flows in a Swirl-Stabilized Model Combustor," *Experiments in Fluids,* Vol. 5, Feb. 1987, pp. 95–102.

[28]Marble, F. E. and Adamson, T. C., Jr., "Ignition and Combustion in a Laminar Mixing Zone," *Jet Propulsion,* Vol. 24, March–April 1954, pp. 85–94.

[29]Griffin, O. M., "Vortex Shedding from Bluff Bodies in a Shear Flow: A Review," *Journal of Fluids Engineering,* Vol. 107, Sept. 1985, pp. 298–306.

[30]Launder, B. E., "Heat and Mass Transport," *Turbulence,* edited by P. Bradshaw, Springer-Verlag, New York, 1978, pp. 231–287.

Recommended Reading from the AIAA Progress in Astronautics and Aeronautics Series . . . AIAA

Dynamics of Explosions and Dynamics of Reactive Systems, I and II

J. R. Bowen, J. C. Leyer, and R. I. Soloukhin, editors

Companion volumes, *Dynamics of Explosions and Dynamics of Reactive Systems, I and II*, cover new findings in the gasdynamics of flows associated with exothermic processing—the essential feature of detonation waves—and other, associated phenomena.

Dynamics of Explosions (volume 106) primarily concerns the interrelationship between the rate processes of energy deposition in a compressible medium and the concurrent nonsteady flow as it typically occurs in explosion phenomena. *Dynamics of Reactive Systems* (Volume 105, parts I and II) spans a broader area, encompassing the processes coupling the dynamics of fluid flow and molecular transformations in reactive media, occurring in any combustion system. The two volumes, in addition to embracing the usual topics of explosions, detonations, shock phenomena, and reactive flow, treat gasdynamic aspects of nonsteady flow in combustion, and the effects of turbulence and diagnostic techniques used to study combustion phenomena.

Dynamics of Explosions
1986 664 pp. illus., Hardback
ISBN 0-930403-15-0
AIAA Members $49.95
Nonmembers $84.95
Order Number V-106

Dynamics of Reactive Systems I and II
1986 900 pp. (2 vols.), illus. Hardback
ISBN 0-930403-14-2
AIAA Members $79.95
Nonmembers $125.00
Order Number V-105

TO ORDER: **Write, Phone, or FAX:** AIAA Order Department, 370 L'Enfant Promenade, S.W., Washington, DC 20024-2518
Phone (202) 646-7444 ■ FAX (202) 646-7508

Sales Tax: CA residents, 7%; DC, 6%. Add $4.50 for shipping and handling. Orders under $50.00 must be prepaid. Foreign orders must be prepaid. Please allow 4 weeks for delivery. Prices are subject to change without notice. Returns will be accepted within 15 days.